

Tuning the Thermotropic and Lyotropic Properties of Liquid-Crystalline Terpyridine Ligands

Franck Camerel,^[a] Bertrand Donnio,^[b] Cyril Bourgoigne,^[b] Marc Schmutz,^[c] Daniel Guillon,^[b] Patrick Davidson,^[d] and Raymond Ziessel*^[a]

Abstract: A rational synthetic strategy is developed to provide compact and simple terpyridine (terpy) mesogens that show liquid-crystallinity both as pure compounds and in organic solution (amphotropic compound). The use of a central 4-methyl-3,5-diacylamino-phenyl platform equipped with two lateral aromatic rings, each bearing three appended aliphatic chains, allows connection of a 2,2':6',2''-terpyridine fragment through a polar group such as an ester, amide, or flat conjugated alkyne linker. For the T¹²ester and T¹²amide scaffolds, the mesophase is best described as a lamellar phase, in which the molecules self-assemble into columnar

stacks held together in layers. In the T¹²amide case, the additional amide link results in significant stabilization of the lamellar phase. The driving forces for the appearance of columnar ordering are the hydrogen-bonding interactions of the amide groups, which induce head-to-tail π -stacking of the terpy subunits. Replacing the polar linker by a nonpolarized but linear alkyne spacer, as in the T¹²ethynyl compound, provides a columnar meso-

phase organized in a rectangular lattice of *p2gg* symmetry. In this arrangement, two nondiscotic molecules arranged into dimers by hydrogen bonding and π - π stacking pile up in a head-to-tail manner to form columns. In addition, the T¹²amide compound proves to be an excellent gelator of cyclohexane, linear alkanes, and DMSO. The resulting robust and transparent gels are birefringent and formed by large aggregates that are readily aligned by shear-flow. TEM and freeze-fracture microscopy reveal that the gels have an original layered morphology made of fibers.

Keywords: amphotropic • gelator • hydrogen bonds • liquid crystals • mesogenic ligand • terpyridine

Introduction


In the last three decades or so, materials science has developed into an interdisciplinary field that makes use of organic, polymeric, and even biological components in addition to the classical metals and inorganics. One of the challenges with this is to endow these materials with desirable or predictable properties such as luminescence, charge transport, and macroscopic ordering in mesophases.^[1–4] In recent years, there has been a tremendous growth in these scientific areas loosely described as materials science and supramolecular chemistry. A wealth of fascinating molecular structures, often involving interlocking complementary molecular moieties, have appeared for possible use in the future development of innovative miniaturized devices.^[5,6] Numerous examples of supramolecular assemblies based on selective metal-to-ligand interactions have been engineered with the goal of forming beautiful and highly symmetrical structures. Elegant strategies have been elaborated to build such assemblies and to provide examples of discrete and infinite helical frameworks,^[7] hydrogen-bonded^[8] or π - π interacting

[a] Dr. F. Camerel, Dr. R. Ziessel
Laboratoire de Chimie Moléculaire
Ecole Chimie, Polymères, Matériaux (ECPM)
Université Louis Pasteur-CNRS (UMR 7509)
25 rue Becquerel, 67008 Strasbourg Cedex (France)
Fax: (+33) 390-242-635
E-mail: ziessel@chimie.u-strasbg.fr

[b] Dr. B. Donnio, Dr. C. Bourgoigne, Dr. D. Guillon
Institut de Physique et Chimie des Matériaux de Strasbourg (IPCMS)
Groupe des Matériaux Organiques (GMO)
Université Louis Pasteur-CNRS (UMR 7504)
23 rue du Loess, BP 43, 67034 Strasbourg Cedex 2 (France)

[c] Dr. M. Schmutz
Institut Charles Sadron, CNRS - UPR 22
6 rue Boussingault, 67083 Strasbourg Cedex (France)

[d] Dr. P. Davidson
Laboratoire de Physique des Solides, Bât. 510
Université Paris-Sud, (UMR 8502 CNRS)
91405 Orsay Cedex (France)

 Supporting information (Complete experimental section including preparation and characterization, DSC traces of T¹²ester and T¹²ethynyl compounds, the XRD pattern of the T¹²ester compound at 180°C) for this article is available on the WWW under <http://www.chemeurj.org/> or from the author.

networks,^[9] three-dimensional complexes displaying defined channels,^[10] cucurbituril assemblies,^[11] highly symmetrical coordination clusters,^[12] and organometallic polymers.^[13]

Many of the new inorganic supermolecules generated over the last few years rely on the coordination of transition-metal cations to polypyridine fragments incorporated into oligomeric ribbons or macroscopic loops.^[14–16] By virtue of forming relatively stable and well-defined complexes with metal cations, such ligands have facilitated the assembly of molecular double- or triple-stranded helicates,^[17,18] catenates,^[19] ladders, and related exotic frameworks,^[20,21] some of them exhibiting useful catalytic,^[22] electronic,^[23] or mesomorphic^[24] properties.

Along these lines 2,2':6',2''-terpyridine (terpy) ligands are particularly attractive because they can form stable complexes with a variety of transition-metal salts.^[25] The result-

ing complexes have many potential applications in fields such as macromolecular chemistry, biochemistry, photophysics, and nanoscience. In particular, terpy and its multiple derivatives have been used advantageously as building blocks for the engineering of novel supramolecular structures such as spiral lines,^[26] dendrimers,^[27] micelles,^[28] polymers,^[29,30] and liquid-crystalline soft materials.^[31] Formation of ordered architectures on surfaces,^[32–34] functional molecular devices,^[35] and biochemical applications^[36] are particularly challenging.

Ruthenium-terpy complexes have received much attention in the field of energy suppliers such as solar cells,^[37] and luminescence devices.^[38,39] Immobilization of terpy ligands and complexes on polymer resins could prove to be of importance in the field of molecular catalysis.^[40]

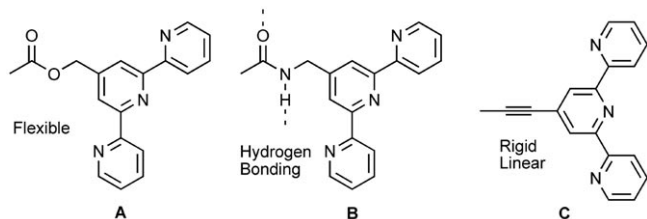
Although terpy ligands offer an enormous structural diversity and tunability in terms of potential properties, stability, and processability, they also typically suffer from a lack of predictability when mesomorphic matter has to be engineered. Multiple strategies have been devised, some of which try to combine a sufficient number of aliphatic chains to control not only the shape and the amphipatic character of the molecule but also the microsegregation process during self-assembly into the mesophase. But this approach remains empirical and lacks rationality. Up to now, only dinuclear metallomesogens involving segmented and bulky terpy ligands appeared to behave as liquid-crystalline materials,^[24] whereas the uncomplexed ligand has remained non-mesomorphic.

One way to overcome these difficulties and to fill the gap of mesomorphic terpy ligands is to engineer a system in which additional intermolecular hydrogen-bonding vectors would stabilize the mesophase.^[41] We chose to synthesize terpy platforms with 1,3-diacylaminobenzene scaffolds to favor intermolecular hydrogen bonding. The introduction of a methyl group bisecting the central phenyl cycle is motivated by the need to tilt the amide vectors out of the plane to extend the dimensionality of the network. Recently, this approach was successfully applied to produce liquid-crystalline phenanthroline ligands and complexes.^[42] From a general point of view acylamino platforms have previously been identified as key elements for the production of liquid-crystalline materials and of efficient gelators of various organic solvents.^[43,44] Some of these gels seem to have great potential as functional soft materials.^[45,46] The gelation of nematic liquid-crystal phases through hydrogen bonding has previously been reported and the gels thus formed have proven to be interesting as dynamic materials in electro-optic devices and as systems responsive to fast stimuli.^[47,48] Recent studies have described terpy-containing carboxylic acids that form hydro-gels, in which hydrogen bonding is provided by an electrostatic interaction induced by proton transfer from the acidic to the basic nitrogen atoms of the terpy ligand.^[49]

As observed in classical liquid-crystalline systems, the shape of the rigid units plays a dominant role in the organization of the molecules during the microsegregation process.^[4,50–54] In our case, it is surmised that the connecting unit

Abstract in French: *Ce travail décrit une synthèse rationnelle des tous premiers ligands mésogènes à base d'unité terpyridine et montre que les propriétés thermotropes et lyotropes de ces composés dépendent notamment du choix du connecteur reliant l'unité terpyridine à l'unité structurante. L'utilisation de l'unité structurante 4-méthyl-3,5-diacylaminophényle équipée de deux cycles aromatiques portant 3 chaînes aliphatiques permet en effet de connecter des sous-unités 2,2':6',2''-terpyridine par l'intermédiaire de groupes polaires tels qu'un ester ou une fonction amide ou encore par le biais d'une connexion apolaire linéaire comme la liaison triple. La mésophase thermotrope obtenue dans le cas des composés T^{12} ester et T^{12} amide est une phase lamellaire dans laquelle les molécules sont organisées par un réseau de liaisons hydrogène en colonne maintenue entre-elles par des interactions secondaires de type π - π au sein des lamelles. Les forces motrices de cette organisation ont été étudiées par spectroscopie infrarouge et par l'étude fine de la structure cristalline d'un composé parent modèle obtenu sur monocristal. L'introduction d'une fonction amide supplémentaire, par le connecteur, résulte dans la stabilisation notoire de cette organisation. Le remplacement des connecteurs polaires par une liaison triple apolaire permet d'obtenir une organisation moléculaire différente aboutissant à la formation d'une mésophase colonnaire de symétrie rectangulaire de type p2gg. Dans cet arrangement, deux molécules, n'impliquant plus les mêmes réseaux de liaisons hydrogène et d'interactions de type π , forment des dimères qui s'empilent tête-bêche pour former des colonnes. De plus, le composé portant trois fonctions amides s'avère être un excellent gélifiant du cyclohexane, des alcanes linéaires et du diméthylsulfoxyde. Les gels obtenus, robustes et transparents, sont biréfringents et constitués d'agrégats pouvant être alignés sous écoulement. Des études par microscopie électronique à transmission effectuées sur des gels dilués mais également des répliques métalliques des gels obtenus après cryofracture révèlent que la formation de ces gels provient de l'auto-organisation en solution de plans formés par juxtaposition parallèle de fibres.*

linking the terpy in the 4'-position of the central ring and the 1,3-diacylaminobenzene will play a prominent role. The use of an ester or an amide dipole will introduce a kink (**A** and **B**), whereas a single nonpolarized triple bond will favor a linear and flat arrangement of the subunits (**C**).^[55] Notice that in the case of the amide linker in **B** additional supramolecular hydrogen bonding is expected to favor the stabilization of the mesophase. The 4'-substitution position was targeted to provide uncrowned ligands likely to π -stack in the solid state.^[56]



In this report, novel thermotropic liquid-crystalline terpy ligands are described and the role of the linker (ester, amide, and ethynyl) is emphasized in light of the data obtained by microscopy, microcalorimetry, and X-ray diffraction.

Results and Discussion

Synthesis: The synthesis of the T^n ester ligands ($n = 8, 12, 16$) was carried out by a convergent strategy outlined in Scheme 1. Starting from ethyl-4-methyl-3,5-diaminobenzoate, the amidation with 3,4,5-trialkyloxybenzoic acid chloride ($n = 8, 12, 16$) and saponification yielded the acid platform bearing two amide functions. Six long aliphatic chains were introduced on the platform to favor mesophase formation. The key esterification step required cross-coupling between this acid platform and the 4'-hydroxymethyl-2,2';6',2''-terpy derivative in the presence of the chloride salt of 1-ethyl-3-[3-(dimethylamino)propyl]carbodiimide (EDC·HCl), under basic conditions provid-

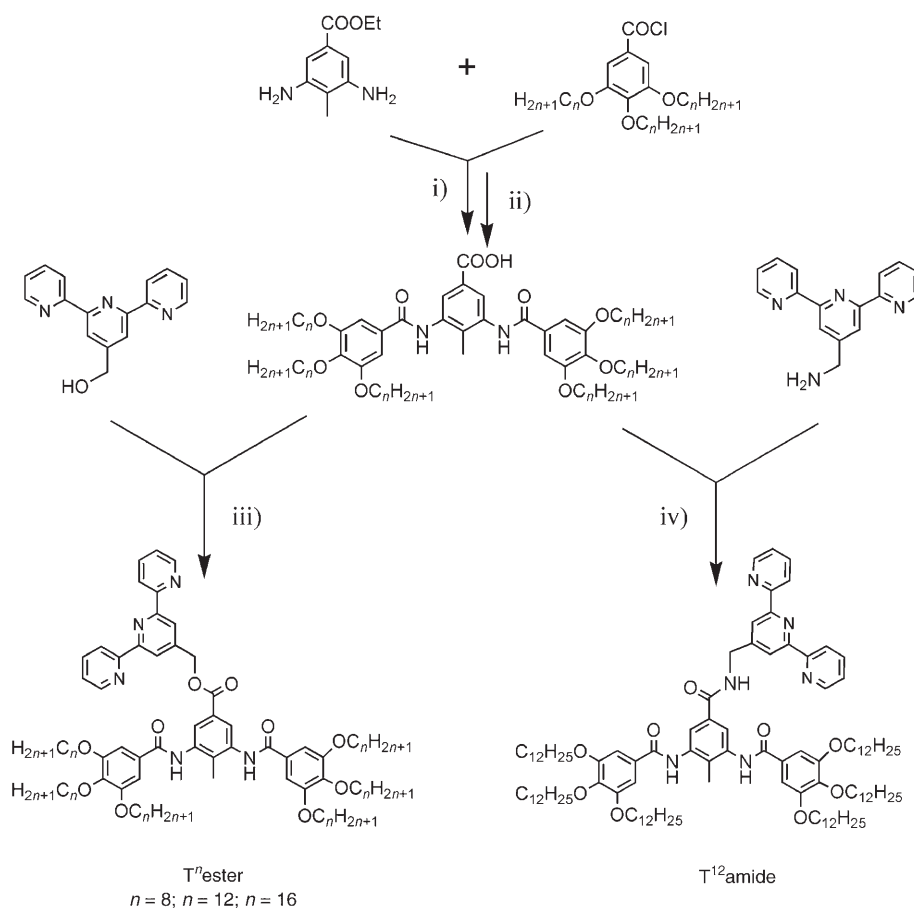
ed by dimethylaminopyridine (DMAP). The trisamide derivative was prepared under similar conditions from 4'-amino-methyl-2,2';6',2''-terpyridine itself synthesized from 4'-methyl-2,2';6',2''-terpyridine^[58-60]

With platforms bearing active functional groups such as iodine,^[61] introduction of 4'-ethynyl-2,2';6',2''-terpyridine^[62] was realized in the presence of catalytic amounts of Pd⁰ (Scheme 2).^[63]

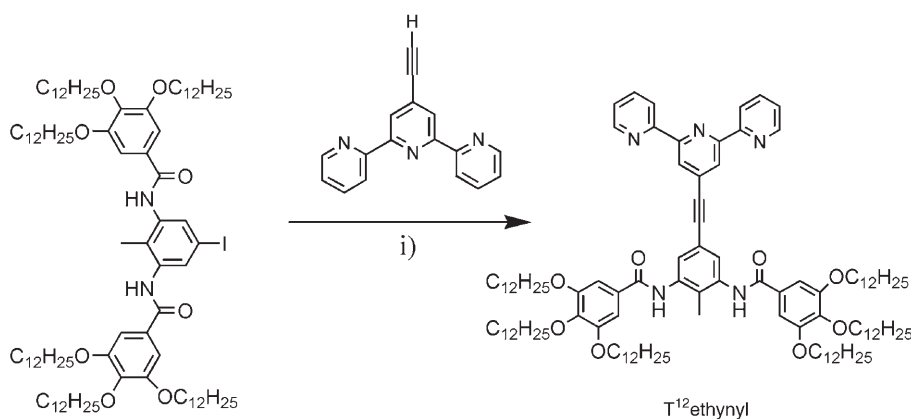
Mesomorphic behavior of the novel terpyridine compounds:

The thermotropic behavior of the terpy ligands was studied by combining thermogravimetric analyses (TGA), differential scanning calorimetry (DSC), polarized optical microscopy (POM), and small-angle X-ray scattering on powder samples (SAXS). These data are summarized in Table 1.

T^n esters: From TGA analyses, the degradation temperature of the compounds was found to be above 225 °C. DSC analyses showed that T^8 ester and T^{16} ester ligands exhibit one single reversible thermal transition at 215 °C and 205 °C, respectively, whereas the T^{12} ester ligand displays two reversible thermal transitions centered at 153 °C and 191 °C on the



Scheme 1. Reagents and conditions: i) anhydrous Na_2CO_3 , acetone, reflux, 82% $n = 8$, 82% $n = 12$, 57% $n = 16$; ii) KOH (50 equiv), THF/ H_2O (v/v), reflux, 85% $n = 8$, 82% $n = 12$, 73% $n = 16$; iii) EDC·HCl (2 equiv), DMAP (1 equiv), CH_2Cl_2 /THF, RT, 76% $n = 8$, 72% $n = 12$, 69% $n = 16$; iv) EDC·HCl (2 equiv), DMAP (2 equiv), CH_2Cl_2 , RT, 56%.



Scheme 2. Reagents and conditions: i) [Pd(PPh₃)₂Cl₂] (6% mol.), (*i*Pr)₂NH, CuI (10% mol) THF, RT, 32%.

Table 1. Thermal behavior of the compounds and X-ray characterization of the mesophases.^[a]

Compound	Transition temperatures [°C] (enthalpy [J g ⁻¹])	<i>d</i> _{meas} [Å]	<i>I</i>	00 <i>l</i>	<i>hk</i>	<i>d</i> _{calcd} [Å]	Mesophase parameters measured at <i>T</i>
T ⁸ ester	Cr 220 I I 215 (-48.6) Cr						
T ¹² ester	L ₁ 162 (4.7) L ₂ 196 (8.5) I I 191 (-8.3) L ₂ 153 (-5.6) L ₁	26.5	VS	001		26.4	<i>T</i> = 120 °C <i>d</i> = 26.4 Å <i>A</i> _M = 121 Å ²
		13.2	M	002		13.2	
		8.8	W	003		8.8	
		7.6	M	B			
		4.6	br	A			
		3.8	br	C			
		26.4	VS	001		26.4	
T ¹⁶ ester	Cr 224 (70.8) I I 205 (-54.7) I	7.5	br	B			<i>T</i> = 180 °C <i>d</i> = 26.4 Å <i>A</i> _M = 127 Å ²
		4.6	br	A			
		3.8	br	C			
T ¹² amide	L ₃ 225 (21.8) I I 225 (21.1) L ₃	26.3	VS	001		26.1	<i>T</i> = 120 °C <i>d</i> = 26.1 Å <i>A</i> _M = 123 Å ²
		13.0	M	002		13.05	
		8.7	W	003		8.7	
		7.5	M	B			
		4.6	br	A			
T ¹² ethynyl	Cr 187 (20.8) PCr 193 (10.0) Col _r 200 (21.0) I I 194.5 (-21.9) Col _r 174 (-12.2) PCr 150 (-7.0) Cr	32.0	VS		20	32.0	<i>T</i> = 198 °C <i>a</i> = 64.1 Å <i>b</i> = 23.6 Å <i>S</i> _{col} = 754.5 Å ²
		22.1	VS		11	22.1	
		15.7	M		31	15.8	
		11.7	M		12	11.6	
		11.1	M		22	11.0	
		7.7	M		42	7.7	
		7.3	M		23/ 13	7.4	
		6.6	W		53	6.7	
		4.7	br		A		
		4.2	br		B		

[a] *d*_{meas} and *d*_{calcd} are the measured and calculated diffraction spacing; *I* is the intensity of the sharp reflections (VS = very strong, M = medium, W = weak); br is used for broad scattering halos; 00*l* and *hk* are the indexations of the reflections corresponding to lamellar and Col phases; *A*_M is the molecular area (*A*_M = *V*_m/*d*); *S*_{col} is the columnar cross section area (*S*_{col} = 1/2*ab*); Cr = crystalline phase; I = Isotropic liquid, Col_r = rectangular columnar mesophase; PCr = poorly crystallized material; L = Lamellar phase. Definitions of *d*_{calcd} and *V*_m are given in the Experimental Section.

first cooling curve (Figure S1, Supporting Information). NMR experiments performed after the DSC measurements revealed that the compounds did not degrade after several

temperature cycles up to 225 °C. For the T⁸ester and T¹⁶ester compounds the single transit was assigned to direct melting into the isotropic liquid at 215 °C and 205 °C for the T⁸ester and T¹⁶ester ligands, respectively. X-ray diffraction patterns obtained for the T⁸ester and T¹⁶ester compounds below these transition temperatures displayed several sharp peaks over the whole 2θ (1° ≤ 2θ ≤ 30°) angular range and confirmed their crystallinity.

At temperatures above 191 °C the T¹²ester ligand is in the isotropic fluid state. On cooling from the isotropic liquid, the material becomes birefringent and fluid and monodomains are observed in the texture under polarized light (Figure 1).

X-ray diffraction patterns obtained for this compound were recorded at various temperatures above and below the thermal transition at 153 °C on cooling from the isotropic melt. The X-ray pattern obtained at 100 °C displayed a diffuse and broad scattering halo A, centered at 4.6 Å in the wide-angle region, indicative of a liquid-like order of the aliphatic chains and thus of the fluid-like nature of the phase (Figure 2). Two other diffuse scattering halos associated with distances of about 7.6 and 3.8 Å (halos B and C), were also observed (halo C is more visible after mathematical deconvolution of the scattered halo A signal). In the small-angle region, the XRD pattern displayed three reflections in a 1:2:3 ratio, which could be indexed as the 001, 002, and 003 reflections of a lamellar phase with a periodicity *d* = 26.4 Å. The scattering

corresponding to C is typical for face-to-face distances between flat aromatic units (here the terpys), the electron density modulation (diffuse band) being short-range. Moreover,

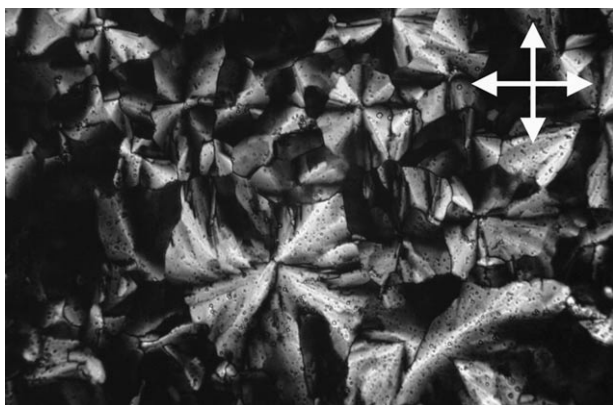


Figure 1. T^{12} ester compound examined by optical microscopy between crossed polarizers upon cooling (symbolized by the cross in the corner of the picture) at 148°C.

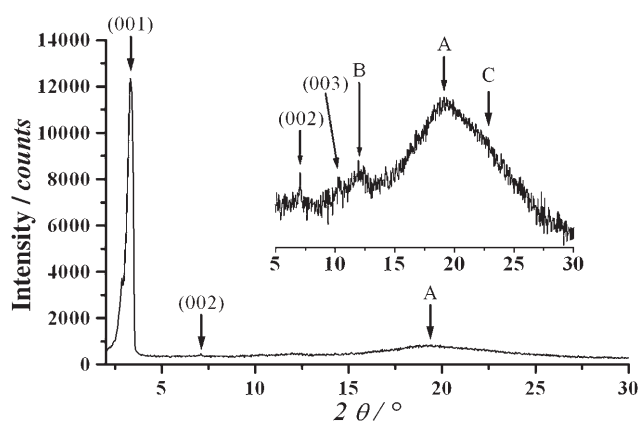


Figure 2. XRD pattern of the T^{12} ester compound at 100°C.

the presence of the diffuse halo B at 7.6 Å (double periodicity) further suggests a short-range, face-to-face, head-to-tail stacking of the molecules, with the central amphipathic 4-methyl-3,5-diacylaminophenyl platforms pointing in opposite directions. In other words, these diffuse signals indicate the existence of short-range ordered columnar piling within the layers. Considering the molecular shape and the occurrence of the diffuse scattering in the wide-angle region, molecular rotation is supposed to be hindered or greatly restricted and is consistent with columnar piling of a dozen molecules (this correlation length is extracted from halo B). At 180°C, the diffraction pattern has the same features (Figure S3, Supporting Information) as those detected at lower temperature in the L_1 phase; the only difference is in the small-angle region, where a single reflection was detected, suggesting a decrease in the molecular order within the lamella (vide infra).

T^{12} amide: TGA measurements performed on the T^{12} amide compound proved thermal stability up to 250°C. DSC traces displayed only one reversible transition at 225°C in heating and cooling cycles. XRD patterns obtained below 225°C revealed that this compound is also liquid crystalline because

they displayed a broad scattering halo (A) centered at ~ 4.6 Å in the wide-angle region, while showing three reflections in the small-angle region (Figure 3). The broad halo A

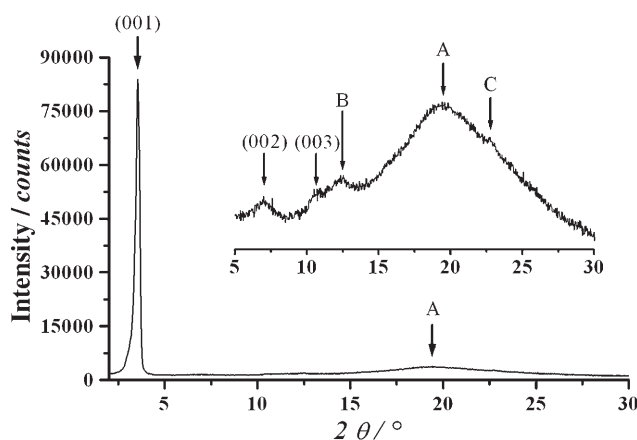


Figure 3. XRD pattern of the T^{12} amide compound at 120°C.

corresponds to the average distance between the molten chains bonded to the ligand. Two slightly less diffuse halos B and C were also observed at 7.5 and 3.8 Å and are attributed to some liquid-like correlations between neighboring molecules, that is, head-to-tail, face-to-face stacking, as for the T^{12} ester described above. Three reflections were observed in the small-angle region and indicate the long-range positional ordering of large objects. The small-angle reflections could be indexed as the fundamental 001 for the sharp and intense reflex and as the 002 and 003 higher-order reflections of a lamellar phase ($d = 26.1$ Å at 120°C). The low intensity of the higher-order reflections 002 and 003, close to the experimental detection limit, results in an apparent broadening of the peaks. The texture observed by polarized optical microscopy below the transition temperature is composed of growing monodomains characteristic of columnar mesophases (Figure 4). Above 225°C, this compound is both fluid and isotropic. The phase transition therefore corresponds to the isotropization of a lamellar liquid-crystalline phase and it appears that this compound is also liquid-crystalline (single-phase) from room temperature to 225°C.

The liquid-crystalline phase observed for the T^{12} amide compound from room temperature to 225°C is similar to that observed for the T^{12} ester compound from room temperature to 153°C. On the basis of the DSC and POM analysis and the XRD analysis, the liquid-crystalline phases observed for T^{12} ester and T^{12} amide compounds can thus be identified as lamellar mesophases constituted of layers containing small columnar aggregates.^[64] It also appears that the substitution of the ester link by an additional binding amide group helps in stabilizing the lamellar phase, as shown by an increase of the isotropization temperature.

T^{12} ethynyl: TGA measurements performed on this compound proved its good thermal stability up to 250°C. The

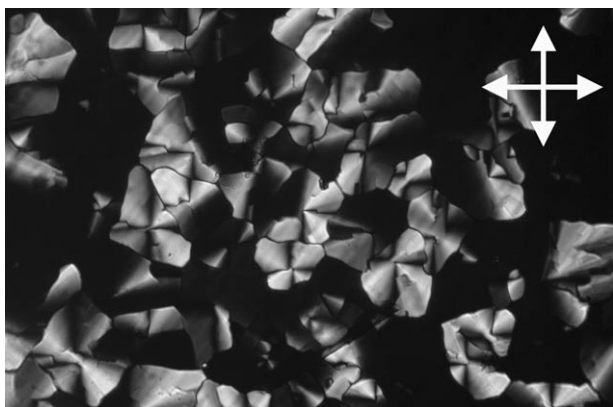


Figure 4. T¹²amide compound viewed by optical microscopy under crossed polarizers (symbolized by the cross in the corner of the picture) at 220 °C.

DSC traces of the T¹²ethynyl displayed three reversible transitions. They are close together in the first heating curve but become well separated on cooling, with an important supercooling effect for the low-temperature transitions (Figure S2, Supporting Information). Above 200 °C, the compound appears fluid and isotropic between crossed polarizers. Cooling from the isotropic liquid, the compound becomes birefringent, and a texture typical of a columnar phase with pseudo-fan shapes is observed (Figure 5a). Between 174 °C and 150 °C, striations appear on the large oriented domains (Figure 5b). Below 150 °C, cracks indicative of a crystalline material are observed (Figure 5c). The second heating curve is identical to the first.

XRD measurements were performed on heating at variable temperatures between 180 and 200 °C by steps of 2 °C. The crystalline nature of the low-temperature phase was confirmed by the XRD patterns obtained below 187 °C, which display sharp peaks in the wide- and small-angle regions. In the temperature range between 187 and 193 °C, sharp peaks were observed in the small-angle region together with a structured broad scattering halo (A) centered at 4.7 Å in the wide-angle region. The structure of this halo corresponds to interference due to the long carbon chains, typical of a poorly crystallized material. XRD patterns, obtained in the 193–200 °C temperature range, displayed a broad scattering halo centered at 4.7 Å (halo A), which proves the fluid-like nature of this phase. In the small-angle region, several sharp peaks were observed, confirming the two-dimensional liquid-crystalline nature of this high-temperature phase (Figure 6). These peaks could be indexed in the *p2gg* rectangular lattice as $(hk) = (20), (11), (31), (12), (22), (42), (23), (13), (33), (53)$ and thus the phase was assigned as a rectangular columnar mesophase (Col_r) with lattice parameters $a = 64.1$ and $b = 23.6$ Å at 198 °C. The halo centered at 4.2 Å (halo B) can be attributed to a mean distance between tilted molecules stacked on top of each other along the columns.

Introduction of an ethynyl junction between the platform and the terpy fragment made the polar part of the molecule

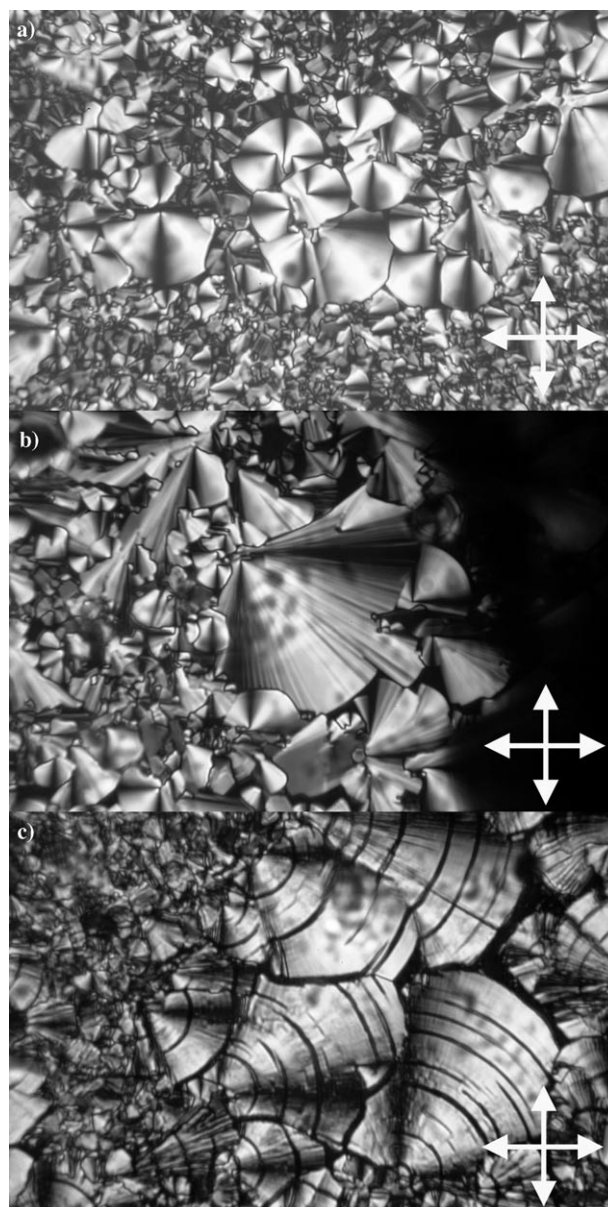


Figure 5. The T¹²ethynyl compound viewed by optical microscopy under crossed polarizers upon cooling (symbolized by the cross in the corner of the picture) at a) 193 °C, b) 165 °C, and c) 133 °C.

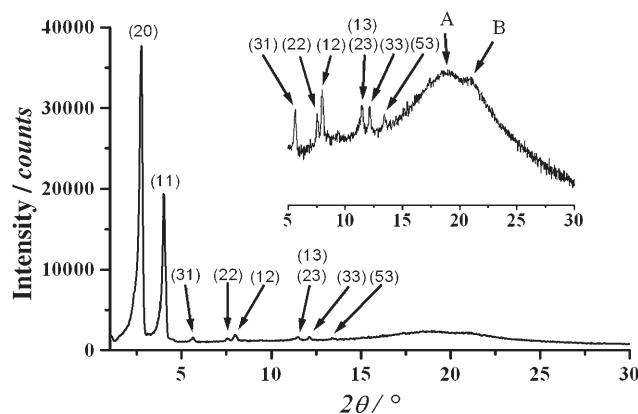


Figure 6. XRD pattern of the T¹²ethynyl compound at 198 °C.

flatter. The angle constraint imposed by the ester and the amide dipole in the Tⁿester and T¹²amide molecules is removed and the molecule can orient the terpy and the central phenyl of the platform in the same plane. However, the more efficient stacking of the polar part of the molecule also increases the rigidity of the system, as clearly shown by the higher transition temperatures, the narrower temperature range of the mesophase, and the stabilization up to 187 °C of the crystalline phase compared to the ester and amide derivatives.

FT-IR spectroscopy: IR spectroscopy is a powerful tool for the study of hydrogen bonds and ordering of hydrocarbon chains in various states of matter. In the present cases (T¹²ester, T¹²amide, T¹²ethynyl), the frequencies of the bands due to CH₂ antisymmetric and symmetric modes (ν_a (CH₂) and ν_s (CH₂)) of the alkyl chains appear at about 2923 and 2852 cm⁻¹ for all three compounds in the mesophase and correspond to some ordering of the hydrocarbon chains with an all-*trans* conformation.^[65,66] However, in dilute CHCl₃ solution, these frequencies shift to 2933 and 2861 cm⁻¹ for all three compounds.

From room temperature to the isotropic melt, all amide dipoles are involved in hydrogen bonding, as clearly evidenced by the ν_{NH} and ν_{CO} stretching vibrations and δ_{NH} deformation vibration, which lie in the 3340–3200, 1678–1651, and 1560–1515 cm⁻¹ ranges, respectively.^[67,68] Notice that corresponding values for the free amides are at 3500–3400 cm⁻¹ for ν_{NH} , around 1680 cm⁻¹ for ν_{CO} , and 1550–1510 cm⁻¹ for δ_{NH} .^[68] For the T¹²ester and T¹²amide compounds, the ν_{NH} bands located at 3331 and 3320 cm⁻¹, respectively, become stronger by cooling the isotropic melt to room temperature. In the T¹²amide case, a broad single stretching vibration at 1666 cm⁻¹ was observed at 220 °C whereas a splitting of this band at 1660 and 1641 cm⁻¹ occurred at 58 °C. The most intriguing situation was found for the T¹²ethynyl compound for which a very weak ν_{NH} band and a large ν_{CO} band centered at 1665 cm⁻¹ were found at 205 °C. Upon cooling from the isotropic melt in the Col_r mesophase at 189 °C, a strong ν_{NH} band at 3207 cm⁻¹ and a sharp ν_{CO} band at 1637 cm⁻¹ were found. The δ_{NH} deformation vibrations were weak but observed in the mesophases at 1520, 1515, and 1507 cm⁻¹ respectively for T¹²ester, T¹²amide, and T¹²ethynyl.

These values are consistent with strong hydrogen bonding involving the amide groups and the absence of free-bonded amides suggests a well-organized state of matter. The high stability and robustness of gels obtained in organic solvents from the T¹²amide compound (vide infra) also suggest a hydrogen-bonded network. By dissolving the T¹²ester and T¹²ethynyl compounds in CHCl₃ (ca. 10⁻³ M) hydrogen bonding is likely to be less effective, as confirmed by the ν_{NH} at 3427/8 cm⁻¹, ν_{CO} at 1673/2 cm⁻¹, and δ_{NH} at 1533/2 cm⁻¹, characteristic of free amide functions.^[69] In marked contrast with these results and in agreement with the increased stability of the mesophases provided by the T¹²amide material is the fact that even at low concentration (<10⁻⁴ M in

CHCl₃) hydrogen bonding is still evident (at 3320 cm⁻¹ for ν_{NH} , at 1660 cm⁻¹ for ν_{CO} , and at 1517 cm⁻¹ for δ_{NH}).

Molecular modeling: To rationalize the molecular organization of these species, in particular within the lamellar mesophases observed for the T¹²ester and T¹²amide compounds, a model inspired by the crystal structure of the homologue T^{OMe}ester compound is proposed. Although the molecular arrangement in the crystalline phase might be different from that in the mesophase, there are nevertheless some features in the mesophase reminiscent of the crystal packing, which may be exploited. The formation of the benzyl amide framework was understood by comparison with the crystal packing of a parent compound of the Tⁿester family in which the six alkoxy terminal chains were replaced by four methoxy groups in the 3,5 positions (T^{OMe}ester).^[70a] This compound crystallizes in the triclinic space group *P* $\bar{1}$ with $a = 8.809(3)$, $b = 12.032(5)$, $c = 16.928(6)$ Å, $\alpha = 79.47(3)$, $\beta = 86.76(3)$, $\gamma = 82.48(3)^\circ$, and $Z = 2$.^[70b] The T^{OMe}ester ligand is nonplanar; the peripheral trisubstituted rings are almost perpendicular to the central phenyl ring while the terpy subunit is tilted by 64° with respect to the central core (Figure 7a). It should be noted that the two amide vectors point in opposite directions, which would favor the formation of a polymeric network. Two remarkable features are evident from the packing of this compound. First, intermolecular hydrogen bonding^[71] is responsible for the formation of a one-dimensional supramolecular edifice (Figure 7b). The tight hydrogen bonds connect the amide groups of a given molecule *L* to its nearest neighbors on top *L'* (NH...O 2.858(37) Å) and bottom *L''* (NH...O 3.097(47) Å) in a centrosymmetric fashion. This strong stabilizing effect forces the terpy fragments to swing out of the hydrogen-bonded stacks. Also present are stabilizing interactions between the almost parallel tetra-substituted phenyl cores with centroid-centroid distances of $L-L' = 5.6$ and $L-L'' = 3.9$ Å.

Second, another interesting feature of the molecular structure is the π - π stacking of the terpy fragments, which runs along the [100] direction between two adjacent one-dimensional, hydrogen-bonded networks. The standard distances between the terpy fragments in the one-dimensional π - π stacks lie in the 3.7 ($L-L''$) and 4.4 Å ($L-L'$) range. This zipping effect leads to the formation of planes strongly stabilized by hydrogen-bonding networks and π - π stacking (Figure 7c).

As mentioned above, the molecule can form both hydrogen bonds through the amide groups and π -stacking through the terpy units. In the crystal packing, a strong directional hydrogen network is visible. Parallel pseudo-columns are formed through the stacking of molecular units in a head-to-tail fashion in order to optimize the hydrogen-bonding interactions. The average distance between two neighboring moieties is about 4.2–4.6 Å, and that between two alternated molecules corresponds to the *a* parameter of the triclinic lattice, $a = 8.8$ Å; the columnar axis is thus aligned along the *a*-direction. These pre-existing pseudo-columns are held together in layers defined by the *b* and *c* parameters, an ar-

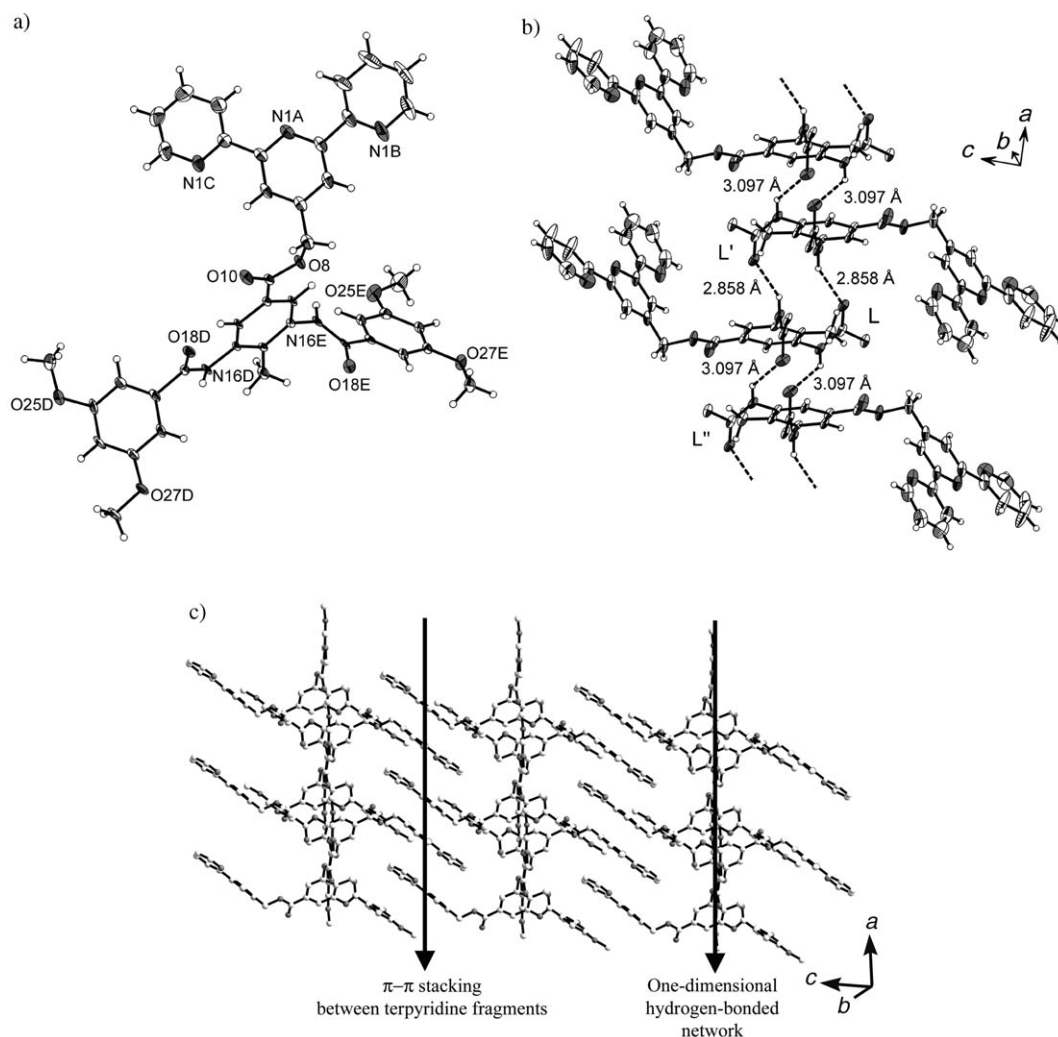


Figure 7. a) Molecular structure of the T^{OMe} ester ligand showing the atom-labeling scheme; b) central trimeric core, setting up the building block of the supramolecular edifice. A single molecule L of T^{OMe} ester (x, y, z) is surrounded by two others ($-x, 1-y, 1-z$] for L' and ($1-x, 1-y, 1-z$) for L'' . The hydrogen bonds (dotted lines) centro-symmetrically connect the amide groups of L to L' ($\text{NH}\cdots\text{O} = 2.858(37) \text{ \AA}$, NHO angle $147(1)^\circ$) and L'' ($\text{NH}\cdots\text{O} = 3.097(47) \text{ \AA}$, NHO angle = $135(1)^\circ$); c) Plane formed by a zipping effect, through π - π stacking between the terpy fragments, of columns of T^{OMe} ester ligands stabilized by hydrogen-bonded networks.

rangement that arises from the interactions between pendant terpy units along the c direction and between the dimethoxyphenyl rings along the b direction. Extrapolation of this packing to describe the molecular organization of the lamellar phase L_1 in the T^{12} ester mesophase thus seems straightforward. Making the assumption that the pseudocolumns are still present, the two distances observed at 3.8 and 7.6 \AA at 120 $^\circ\text{C}$ or 3.8 and 7.5 \AA at 180 $^\circ\text{C}$ suggest an alternated stacking of the terpy fragments reminiscent of the crystalline structure. The chains are thus confined to the two opposite quadrants perpendicular to the columnar hard core, preventing the stacking of the trialkoxyphenyl units, whereas the terpys occupy the free volume left and are still available for π -stacking interactions. This particular organization allows for the lateral interactions of the columns, which are forced to lie parallel and confined in well-defined layers (Figure 8). The layers are separated from each other

by a dense aliphatic continuum that is responsible for the loss of intercolumnar interactions in the third direction (b direction), precluding a columnar phase with two-dimensional symmetry. This arrangement is compatible with the spacing periodicity deduced from XRD (26.0 \AA versus 32.0 \AA in the model) and is also in agreement with the molecular area ($6 \times 21 \text{ \AA}^2$). In order to compensate the surface generated by the formation of this rigid plane, the chains ought to be in a very disordered state, likely with some interdigitation. The formation of the L_2 phase at higher temperatures likely corresponds to the partial loss of such a molecular arrangement, which probably results from a decrease of the stacking interactions and an increase of the molecular diffusion owing to the thermal fluctuations and from the larger volume required by the aliphatic chains.^[72] The same description can be used for the T^{12} amide mesophase, which exhibits the same structural features. Moreover, in view of

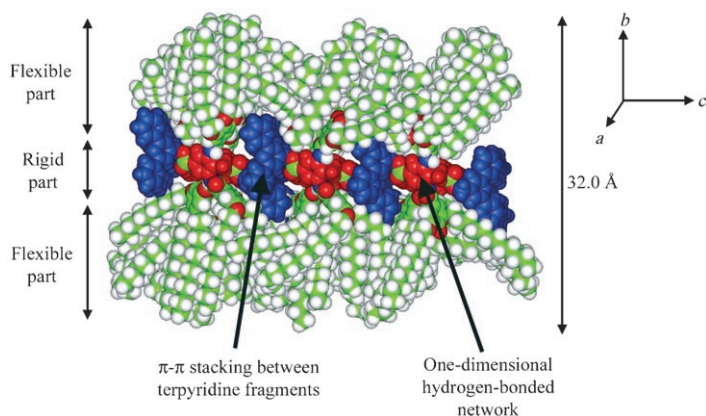


Figure 8. Molecular modeling of the layer observed in the mesophases of the T¹²ester and T¹²amide compounds, based on the T^{OMe}ester crystallographic structure.

this, it is now clear why the triamide derivative exhibits a single lamellar phase (L₃), the hydrogen-bonding interactions being much stronger in this case than for the ester-diamide compound, inhibiting a random stacking. This is clearly confirmed by the FT-IR measurements in the various states of matter (vide supra).

For the ethynyl derivative the columnar cross-section in the Col_r mesophase is not circular and the particular arrangement of the elliptical columnar cross-sections leads to a rectangular lattice. Such an elliptical shape can be generated if two molecules are arranged into head-to-tail dimers, with the terpy unit now located in the same plane as depicted in Figure 9a. These dimers stack on top of each other to form columns but unlike the previous situation, the columns do not possess any particular lateral registry, and these columns are arranged into a rectangular lattice. The same types of interactions are responsible for the formation of the mesophase as for the ester and amide compounds: hydrogen bonding and π - π stacking. Molecular dynamic calculations confirmed that such dimers can be perfectly organized into a rectangular lattice of *p2gg* symmetry with $a = 64.1$ Å and $b = 23.6$ Å and an occupancy density of 0.9 (Figure 9b).

The proposed models of these novel, self-organized materials are in keeping with the attribution of the broad peaks found in the X-ray diffraction patterns for T¹²ester and T¹²amide (A: 4.6 Å; B: 7.6 Å; C: 3.8 Å), as well as for T¹²ethynyl (A: 4.7 Å; B: 4.2 Å). Of particular interest is peak C, attributed to stacking of the terpyridine subunits as unambiguously found in the molecular structure determined by analysis of single crystals. The X-ray crystal structure clearly shows the head-to-tail stacking of the terpyridine units with a double distance corresponding to the antiparallel stacking periodicity (expected, since the molecules are not symmetrical). Therefore, it is reasonable to suppose that the liquid-crystal mesophase of T¹²ester and T¹²amide compounds partly retains some of the structural features of the crystalline phase of the parent compound T^{OMe}ester. Owing to the dynamics and the fluidity of the phase, the peaks are broadened, which means that the order is short range. The

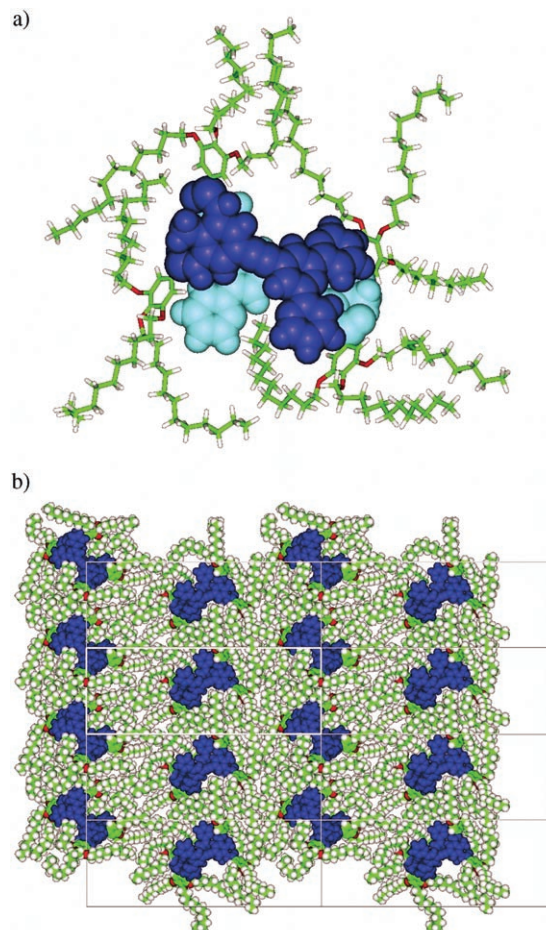


Figure 9. a) Dimer constructed from two head-to-tail T¹²ethynyl molecules; b) two-dimensional rectangular unit cell of *p2gg* symmetry built with the head-to-tail dimer of the T¹²ethynyl compound ($a = 64.1$ Å; $b = 23.6$ Å).

shift of the reflection in the case of the ethynyl compound (peak B) to longer distances indicates a tilt of the molecular plane (plateau) with respect to the axis of the columns. This tilt also implies that the second harmonic is dramatically weak and consequently not visible. This is a common observation in columnar liquid crystal phases.

Gelation properties of the T¹²amide compound: Since amphiphilic molecules built on a 1,3,5-benzenetricarboxamide core are known to be good gelators for organic solvents,^[43,44,73] the gelation abilities of the T¹²amide compound were evaluated in various polar and nonpolar, protic and nonprotic solvents. This terpy derivative induced gelation of cyclohexane, linear alkanes from C₆ to C₁₂, and dimethyl sulfoxide (DMSO). Robust and transparent gels were formed in cyclohexane and in linear alkanes at 25 °C after heating a mixture of the ligand and the solvent to form a homogeneous fluid solution. Upon cooling below the gelation temperature, the complete volume of solvent is immobilized and can support its own weight without flowing as shown in Figure 10a. The organogels exhibited thermally reversible sol/gel transitions. The minimum gelation concentrations ob-

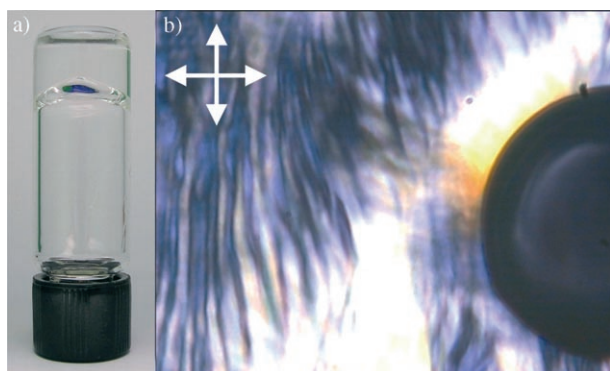


Figure 10. a) Gelation test in cyclohexane of the T¹²amide compound in cyclohexane (2.6% (w/w)). Gel formation is confirmed if the sample does not flow in a few hours after the test tube is turned upside-down. b) Texture of a gel of T¹²amide in cyclohexane ($c = 20.85\%$ (w/w)) observed by optical microscopy between crossed polarizers (the black area corresponds to an isotropic air bubble). The crossed polarizers are symbolized by the white arrows in the top left corner of the picture.

served (MGC, hexane: 0.55% (w/w); cyclohexane: 0.55% (w/w); dodecane: 0.44% (w/w); DMSO: 1.32% (w/w)) showed that these mesogenic ligands displayed good gelation abilities, comparable to those already reported for other low-molecular-weight organogelators.^[74] The role of hydrogen bonding was confirmed by infrared spectroscopy experiments performed with the cyclohexane gel. Two C=O stretching bands were observed at 1641 and 1660 cm^{-1} and a single NH stretching vibration at 3279 cm^{-1} . These spectroscopic data are an unambiguous signature of hydrogen-bonded amides inducing a hydrogen-bonded network. It should be noted that transparent gels can also be formed with the T¹²ester compound—but at higher concentration (MGC, cyclohexane: 1.3% (w/w))—and that only turbid gels are formed with the T¹²ethynyl compound.

Observations by optical microscopy between crossed polarizers proved that the gels of the T¹²amide compound are strongly birefringent, which suggests that they form a lyotropic liquid-crystalline phase (Figure 10b). SAXS experiments were therefore performed with gels of the T¹²amide compound in cyclohexane. The SAXS intensity was easily observed, even at the rather low concentration of 12% (w/w), and the SAXS pattern (Figure 11a) of a well-aligned sample has an anisotropic “butterfly” shape. This pattern is typical of a single domain of nematic phase comprised of large aggregates aligned by the shear-flow that occurs when the X-ray capillary is filled with sample. The scattered intensity regularly decreases with increasing scattering angle, which suggests that the aggregates are randomly located (no positional order), since no diffraction peak can be detected. In contrast, the SAXS pattern (Figure 11b) of a 21% (w/w) mixture showed an anisotropic diffuse peak located at $q = 0.134 \text{ \AA}^{-1}$. The diffuse peak corresponds to a liquid-like order of the aggregates with an average distance of 74 \AA between them. Even though this scattering data proves that the mechanical properties of the gels arise from the existence of large aggregates, this data does not allow us to

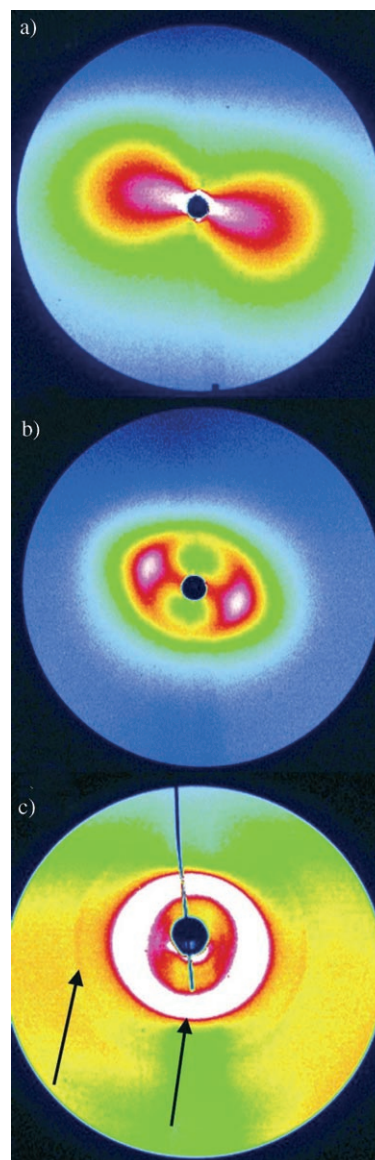


Figure 11. SAXS two-dimensional scattering patterns obtained with gels of the T¹²amide compound at various concentrations: a) 12% (w/w); b) 21% (w/w); and c) 38% (w/w). The black arrows point to the diffraction lines.

identify their nature. More information can be obtained from electron microscopy images of these gels (see below). The SAXS pattern (Figure 11c) of a gel of even higher concentration, 38% (w/w), displays three sharp diffraction lines at scattering vectors of 0.235 \AA^{-1} , 0.404 \AA^{-1} , and 0.47 \AA^{-1} in ratios 1, $3^{1/2}$, and 2. These diffraction lines prove that the T¹²amide compound stacks in columns that self-assemble on a hexagonal lattice with a parameter of $a = 49 \text{ \AA}$ at this concentration. The gels thus clearly form a lyotropic hexagonal columnar mesophase.

TEM experiments were performed to examine the morphology of these gel materials and the nature of the large objects that induce the gelation. Images obtained from very dilute solutions of T¹²amide ligand in cyclohexane (0.04% (w/w)) dried onto a carbon-coated grid reveal the presence

of very thin fibers (2 nm thick and several μm long) (long arrow on Figure 12a). An interesting feature is that the diameter of these fibers is monodisperse. The fibers also show a tendency to associate locally to form sheets in this dried state (short arrow). To directly examine the morphology of these fibers in the gel state, freeze-fracture electron microscopy (FFEM) experiments were performed on gels of the T^{12} amide compound in cyclohexane ($C > 0.55\%$ (w/w)). In the gels, a clear lamellar structure was observed, which consists of extended layers (several micrometers) of less than 10 nm in thickness (Figure 12b). The organic layers regularly stack to form large, randomly oriented lamellar domains. Inside the layers fine striations are seen, which correspond

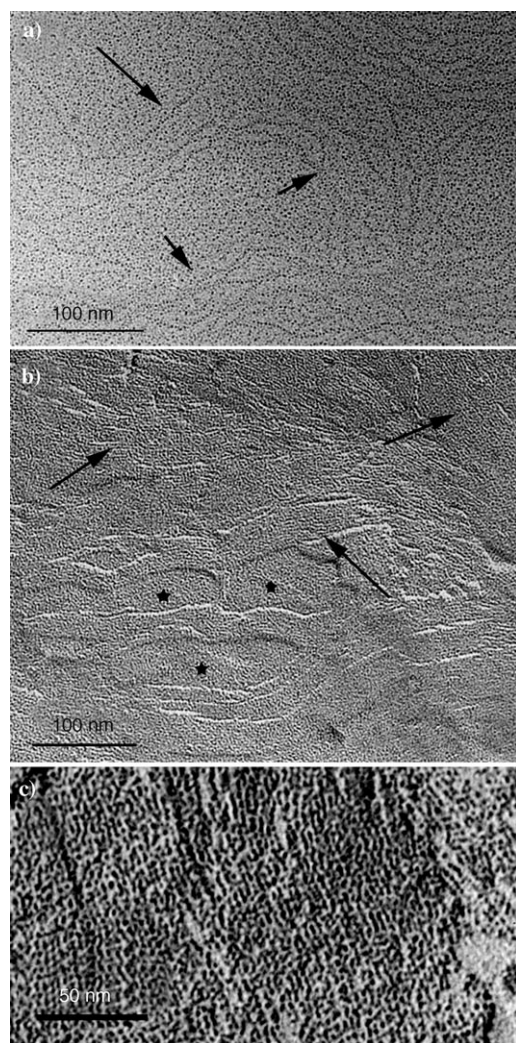


Figure 12. a) Image obtained by TEM of a very dilute solution of the T^{12} amide compound in cyclohexane ($c = 0.04\%$ (w/w)) showing thin fibers (2 nm thick and several μm long) (long arrow). The fibers show a tendency to associate to form sheets (short arrow). The black dots visible in the figure are the Pt particles seen at high magnification. b) Lamellar structure as observed by FFEM of a gel of T^{12} amide compound in cyclohexane ($c = 2.6\%$ (w/w)). The observed layers display fine striations corresponding to the individual fibers observed in diluted solution (arrow) in a highly compacted state. The stars point to solvent areas trapped between the layers. c) Image obtained by FFEM clearly showing the regular aggregation of the fibers into layers (interfiber distance = 4 nm).

to the individual fibers observed in dilute solution (arrow) in a highly compacted state. These fibers are self-assembled into layers with a regular distance of 4 nm (Figure 12c). The stars likely correspond to solvent areas trapped in between the layers. It appears that the compound is not a classical organogelator for which the formation of a three-dimensional network of entangled, fiber-like aggregates is responsible for the immobilization of the solvent.^[43,44,73–75] These microscopic observations reveal that the gel formation in this case arises from the self-assembly of lamella in solution (lyotropic system).

TEM experiments confirm the presence of large objects in solution. Below the minimum concentration for gelation (MGC), the formation of fibers, monodispersed in diameter, prevails. Above the MGC, the aggregation of these fibers into layers is responsible for gelation. The organization of the layer observed in the gel is probably close to that of the thermotropic mesophase of the T^{12} amide compound. From IR experiments, it was demonstrated that hydrogen-bonded amides play a role in the gel formation. Comparison with the thermotropic mesophase suggests that the fibers are developed through an extended one-dimensional network of hydrogen bonds and these fibers are associated through π - π stacking between the terpy fragments in solution to form layers. TEM pictures obtained at various concentrations also reveal that the compactness of the layer, that is, the distance between the fibers, remains constant. Since the distance determined by SAXS decreases when concentration increases, the peak observed on the diffraction pattern can be associated to interference between the layers. The anisotropy of the SAXS patterns corresponds to the alignment of the layers along the flow, that is, the long axis of the capillary, induced when the capillary was filled.^[76] At high concentration, when the interlayer distance is close to the distance between the fibers within the layer (~ 4 nm), the packing of the layers leads to the formation of a hexagonal array. These microscopic observations and SAXS experiments reveal that the formation of these gels is certainly induced by the self-assembly of lamella stabilized by hydrogen bonding and π - π stacking interactions as observed in the thermotropic liquid-crystalline state.^[77]

Conclusion

Our results show that substitution of terpy frameworks with a 4-methyl-3,5-diacylaminobenzene core equipped with two secondary amide functions, each carrying a phenyl ring with three paraffin chains, induces the occurrence of liquid-crystalline properties. The nature of the group linking the terpy to the platform and the length of the aliphatic chains play crucial roles in the formation of the thermotropic mesophases. For the T^n ester family, the octyloxy and hexadecyloxy derivatives were not mesomorphic, whereas the dodecyloxy compound exhibited mesomorphism from room temperature to 191 °C. Most significantly, the T^{12} amide compound is mesomorphic from room temperature to 225 °C, extending the

mesomorphic domain by 34°C. In the cases of the T¹²ester and T¹²amide compounds, a lamellar phase containing columnar aggregates was observed. Replacing the ester or amide link by a triple bond in the T¹²ethynyl compound narrowed the mesomorphic domain to 20.5°C between 194.5 and 174°C on cooling. X-ray scattering confirmed the existence of a columnar mesophase with rectangular symmetry.

Based on the crystal structure of a model compound (bearing methoxy groups in place of the aliphatic chains), we suggest that the lamellar mesophase of the T¹²ester and T¹²amide derivatives is formed by an alternated organization of the terpy subunits stabilized by π - π stacking interactions and hydrogen bonding reminiscent of pseudocolumns, in which all alkyl chains are pushed to both sides of the layer. For the more rigid molecule bearing a conjugated ethynyl spacer, the favorable orientations of the terpy and the central phenyl in the same plane induce a spatial arrangement involving head-to-tail dimers, elliptical in shape. Stacking these dimers gives rise to the formation of columns. In all three cases, the amide functions are clearly involved in a supramolecular, hydrogen-bonded network, as deduced from infrared studies and X-ray diffraction studies on single crystals of a model compound. A remarkable feature of the T¹²amide derivative is the gelation of hydrocarbon solvents and DMSO. TEM measurements and SAXS experiments reveal that this compound is not a classical organogelator; instead, the gel is likely formed from one-dimensional swelling of a lamellar phase. Furthermore, it appears that the supramolecular organization in solution is reminiscent of the lamellar organization of the pure compounds, combining hydrogen bonding between the amide functions and π - π stacking interactions between the aromatic moieties of the molecules. FFEM experiments allow us to conclude that the layers are formed from self-assembled fibers.

The original design and synthesis of molecules (new amino terpyridine) together with an interplay of crystal structure, temperature-dependent infrared studies in the bulk samples, X-ray diffraction in the solid and liquid-crystalline phases, molecular modeling, organogel formation (SAXS on gels), lyotropic properties, and electron microscopy (freeze-fracture and classical TEM) allow us to present these unconventional mesomorphic compounds. The multidisciplinary aspect of this work will be pursued further by complexation of the empty coordination site with transition metals in order to endow the resulting material with interesting electronic or optical properties. Work is currently in progress along these lines.

Experimental Section

General: The 300 and 200 (¹H), and 75.47 MHz (¹³C) NMR spectra were recorded at room temperature with perdeuterated solvents; residual protonated solvent signals provided internal references. Differential Scanning Calorimetry (DSC) was performed on a Perkin-Elmer DSC-7 instrument at a scanning rate of 10 Kmin⁻¹. ThermoGravimetric Analyses (TGA) were performed on an SDTQ 600 apparatus at a scanning rate of 10 Kmin⁻¹ under argon. Phase behavior was studied by means of polar-

ized light optical microscopy (POM) on a Leitz microscope equipped with a Mettler-Toledo FP80 hot-stage and an FP80 central processor. X-ray scattering measurements were carried out with two different experimental setups. In both cases, a linear monochromatic Cu_{K α} beam ($\lambda = 1.5405 \text{ \AA}$) was obtained using a sealed-tube generator (900 W) equipped with a bent monochromator. In the first set, the transmission Guinier geometry was used, whereas a Debye-Scherrer like geometry was used in the second experimental setup. In all cases, the crude powder was filled in Lindemann glass capillaries of 1 mm diameter and 10 μm wall thickness. Small-angle X-ray scattering experiments with gel samples were performed with laboratory setups described in detail below. Samples were held in cylindrical Lindemann glass capillaries of 1 mm diameter and 10 μm wall thickness. UV/Vis spectra were recorded using a UVIKON 940/941 dual-beam grating spectrophotometer (Kontron Instruments) with a 1 cm quartz cell. FT-IR spectra were recorded using a Perkin-Elmer "spectrum one" spectrometer on the neat liquids or thin films, prepared with a drop of dichloromethane and evaporated to dryness on KBr pellets. The molecular-modeling calculations were performed on an SGI Origin 200 4 CPU computer and on an SGI Octane2 workstation using the DISCOVER 3 molecular mechanics package from Accelrys (www.accelrys.com) with the pcff force field. Transmission electron microscopy (TEM) experiments were performed with a CM12 Philips microscope on dilute solution deposited onto a carbon-coated grid and on metallic replicas of the gels obtained by the freeze-fracture technique.

T¹²ester: 3,5-Bis(3,4,5-tridodecyloxybenzoylamino)-4-methyl benzoic acid (0.500 g, 0.338 mmol), dimethylaminopyridine (DMAP) (0.041 g, 0.338 mmol), and distilled CH₂Cl₂ (20 mL) were introduced in a Schlenk flask under argon. After complete solubilization of the acid under stirring, 1-[3-(dimethyl-amino)propyl]-3-ethylcarbodiimide hydrochloride (EDCI, 0.065 g, 0.338 mmol) and 4'-hydroxymethyl-2,2';6',2''-terpyridine (0.089 g, 0.338 mmol) were added to the clear solution. This mixture was stirred at room temperature overnight. After removal of the solvent, purification of the product was performed by flash chromatography on silica gel with CH₂Cl₂/MeOH (99:1 to 98:2), followed by crystallization from CH₂Cl₂/CH₃CN, yielding 0.420 g (72%). ¹H NMR (CDCl₃, 200 MHz): $\delta = 0.87$ (t, ³J = 6.3 Hz, 18H; CH₃), 1.27 (m, 108H; CH₂), 1.76 (m, 12H; CH₂), 2.14 (s, 3H; CH₃), 3.93 (m, 12H; OCH₂), 5.42 (s, 2H; OCH₂), 7.09 (s, 4H; H arom.), 7.30 (m, 2H; CH), 7.82 (td, ³J = 7.8, ⁴J = 1.8 Hz, 2H; CH), 8.11 (s, 2H; CH), 8.38 (s, 2H; CH), 8.59 ppm (m, 6H; CH+NH); ¹³C{¹H} DEPT NMR (75.47 MHz, CDCl₃): $\delta = 14.02$ (CH₃), 14.10 (CH₃), 22.69 (CH₂), 26.10 (CH₂), 29.38 (CH₂), 29.46 (CH₂), 29.63 (CH₂), 29.67 (CH₂), 29.70 (CH₂), 29.73 (CH₂), 29.77 (CH₂), 30.36 (CH₂), 31.93 (CH₂), 65.25 (OCH₂), 69.23 (OCH₂), 73.48 (OCH₂), 106.01 (CH), 119.21 (CH), 121.43 (CH), 123.90 (CH), 124.37 (CH), 136.82 (CH), 148.95 (CH), 127.81 (Cq), 128.88 (Cq), 133.93 (Cq), 136.86 (Cq), 141.51 (Cq), 146.96 (Cq), 153.11 (Cq), 155.66 (Cq), 155.81 (Cq), 165.20 (C=O), 166.31 ppm (C=O); IR (KBr): $\tilde{\nu} = 3437$ (ν NH), 3261 (ν NH), 2923 (ν CH), 2853 (ν CH), 1728 (ν COO), 1638 (ν CO), 1617 (ν CO), 1584 (ν C=C), ν C=N), 1519 (δ NH), 1490, 1468, 1426, 1407, 1384, 1337, 1275, 1263, 1235, 1214, 1114, 1072, 1041 cm⁻¹; UV/Vis (CH₂Cl₂, 23°C): λ_{max} (ϵ) = 277 (73 700), 252 (66 800 m⁻¹cm⁻¹); MS (FAB+, mNBA): m/z (%): 1725.2 (100) [M^+ +H]; elemental analysis calcd (%) for C₁₁₀H₁₇₃N₃O₁₀: C 76.56, H 10.11, N 4.06; found: C 76.41, H 10.02, N 3.98.

T¹²amide: A Schlenk flask equipped with a septum and an argon inlet was charged with 3,5-bis(3,4,5-tridodecyloxybenzoylamino)-4-methylbenzoic acid (0.35 g, 1.1 equiv, 0.23 mmol) in distilled CH₂Cl₂ (50 mL) and dimethylaminopyridine (DMAP, 0.06 g, 2.2 equiv, 0.47 mmol), and the mixture was stirred until the acid was completely dissolved. 1-[3-(dimethyl-amino)propyl]-3-ethylcarbodiimide hydrochloride (EDCI, 0.09 g, 2.2 equiv, 0.47 mmol) and 4'-aminomethyl-2,2';6',2''-terpyridine (0.06 g, 1 equiv, 0.21 mmol) were added to the clear solution, which was stirred overnight. After evaporation of the solvent, purification was performed by flash chromatography on silica gel with CH₂Cl₂/MeOH (99.9:0.1 to 98:2), followed by crystallization from CH₂Cl₂/CH₃CN to yield 0.20 g (56%). ¹H NMR (CDCl₃, 300 MHz): $\delta = 0.89$ (t, ³J = 4.5 Hz, 18H; CH₃), 1.26 (m, 108H; CH₂), 1.72 (m, 12H; CH₂), 2.21 (s, 3H; CH₃), 3.95 (m, 12H; OCH₂), 4.40 (d, ³J = 3.96 Hz, 2H; CH₂), 7.20 (m, 6H; H arom.), 7.66 (td, ³J = 7.7, ⁴J = 1.7 Hz, 2H; CH), 7.90 (s, 2H; CH), 8.01 (s, 2H; CH), 8.26 (d, ³J = 7.9 Hz, 2H; CH), 8.49 (d, ³J = 4.3 Hz, 2H;

CH), 8.65 ppm (s, 3H; NH); $^{13}\text{C}\{^1\text{H}\}$ DEPT NMR (75.47 MHz, CDCl_3): $\delta = 13.69$ (CH_3), 14.10 (CH_3), 22.69 (CH_2), 26.10 (CH_2), 26.16 (CH_2), 29.38 (CH_2), 29.47 (CH_2), 29.62 (CH_2), 29.66 (CH_2), 29.72 (CH_2), 29.75 (CH_2), 30.36 (CH_2), 31.93 (CH_2), 69.16 (OCH_2), 73.43 (OCH_2), 105.94 (CH), 119.14 (CH), 121.55 (CH), 123.09 (CH), 123.97 (CH), 136.85 (CH), 148.93 (CH), 128.82 (Cq), 132.00 (Cq), 137.02 (Cq), 141.27 (Cq), 148.66 (Cq), 152.24 (Cq), 153.08 (Cq), 154.98 (Cq), 155.53 (Cq), 165.88 (C=O), 168.02 ppm (C=O); IR (KBr): $\tilde{\nu} = 3437$ (νNH), 3271 (νNH), 2923 (νCH), 2853 (νCH), 1640 (νCO), 1584 ($\nu\text{C}=\text{C}$, $\nu\text{C}=\text{N}$), 1521 (δNH), 1494, 1468, 1426, 1406 (νCH_2), 1384, 1334, 1263, 1232, 1115 cm^{-1} ; UV/Vis (CH_2Cl_2 , 23 °C): λ_{max} (ϵ) = 277 (107700), 252 (96600 $\text{m}^{-1}\text{cm}^{-1}$); MS (FAB+, mNBA): m/z (%): 1724.2 (100) [M^+ +H]; elemental analysis calcd (%) for $\text{C}_{110}\text{H}_{174}\text{N}_6\text{O}_9$: C 76.61, H 10.17, N 4.87; : C 76.52, H 10.04, N 4.75.

T¹²ethynyl: A Schlenk flask was charged with 2,6-bis(3,4,5-tridodecyloxybenzoylamino)-4-iodo-toluene (0.500 g, 0.32 mmol), 4'-ethynyl-2,2':6',2''-terpyridine (0.082 g, 0.32 mmol), $[\text{Pd}(\text{PPh}_3)_2\text{Cl}_2]$ (0.014 g, 0.02 mmol), THF (50 mL), and $i\text{Pr}_2\text{NH}$ (5 mL). The mixture was thoroughly degassed with argon. CuI (0.013 g, 0.06 mmol) was added and the mixture was stirred at room temperature for 24 h. The organic phase was filtered over celite, washed with water (150 mL), and dried over MgSO_4 . After removal of the solvent, chromatography on silica gel treated with triethylamine (cyclohexane/ CH_2Cl_2 gradient from 80:20 to 0:100) afforded the pure compound (0.170 g, 32%). ^1H NMR (200.1 MHz, CDCl_3): $\delta = 0.87$ (m, 18H; CH_3), 1.1–1.6 (m, 108H; CH_2), 1.7–1.9 (m, 12H; CH_2), 2.24 (s, 3H; CH_3), 4.02 (t, $^3J = 6.05$ Hz, 12H; OCH_2), 7.13 (s, 4H), 7.32 (m, 2H), 7.67 (s, 2H), 7.84 (td, $^3J = 7.7$ Hz, $^4J = 1.7$ Hz, 2H), 8.04 (s, 2H), 8.48 (s, 2H), 8.56 (d, $^3J = 7.8$ Hz, 2H), 8.67 ppm (d, $^3J = 4.0$ Hz, 2H); $^{13}\text{C}\{^1\text{H}\}$ DEPT NMR (75.47 MHz, CDCl_3): $\delta = 13.5$ (CH_3), 14.1 (CH_3), 22.7 (CH_2), 26.1 (CH_2), 29.4 (CH_2), 29.6 (CH_2), 29.7 (CH_2), 30.4 (CH_2), 31.9 (CH_2), 69.4 (OCH_2), 73.6 (OCH_2), 106.0 (CH), 121.2 (CH), 122.9 (CH), 123.9 (CH), 125.6 (CH), 136.8 (CH), 149.2 (CH), 87.8 (Cq), 92.9 (Cq), 120.87 (Cq), 128.0 (Cq), 129.1 (Cq), 133.2 (Cq), 136.7 (Cq), 141.7 (Cq), 153.3 (Cq), 155.5 (Cq), 155.7 (Cq), 165.9 ppm (C=O); IR (KBr): $\tilde{\nu} = 3400$ (νNH), 3194 (νNH), 2915, 2852, 1638 (νCO), 1607, 1583, 1517 (δNH), 1493, 1467, 1426, 1391, 1337, 1264, 1233, 1114, 1067, 1041 cm^{-1} ; UV/Vis (CH_2Cl_2 , 23 °C): λ_{max} (ϵ) = 254 (53910), 284 (77110 $\text{m}^{-1}\text{cm}^{-1}$); MS (FAB+, mNBA): m/z (%): 1691.2 (100) [M^+ +H]; elemental analysis calcd (%) for $\text{C}_{110}\text{H}_{171}\text{N}_5\text{O}_8$: C 78.10, H 10.19, N 4.14; found: C 77.90, H 9.83, N 3.93.

Acknowledgements

This work was supported by the University Louis Pasteur (ULP), the School of Chemical Engineering (ECPM), and the CNRS. We gratefully acknowledge Dr. Benoît Heinrich for his skilled assistance and helpful discussions, and Clément Vuilleumier who took an active part in the SAXS experiments on gels. We thank Dr. P. Schultz for the use of the cryofracturing apparatus developed by Dr. J.-C. Homo at the IGBMC UMR 7104, Illkirch, France.

- [1] J.-M. Lehn, *Supramolecular Chemistry*, VCH, Weinheim, **1995**.
- [2] a) R. Ziessel, M. Hissler, A. El-ghayoury, A. Harriman, *Coord. Chem. Rev.* **1998**, *180*, 1251–1298; b) V. Ramamurthy, K. S. Schanze, *Multimetallic and Macromolecular Inorganic Photochemistry*, Marcel Dekker, New York, **1999**.
- [3] a) P. Haisch, G. Winter, M. Hanack, L. Lüer, H.-J. Egelhaai, D. Oelkrug, *Adv. Mater.* **1997**, *9*, 316–321; b) A. M. Van de Craats, J. M. Warman, A. Fechtenkötter, J. D. Brand, M. A. Harbison, K. Müllen, *Adv. Mater.* **1999**, *11*, 1469–1472.
- [4] a) J. L. Serrano, *Metallomesogens*, VCH, Weinheim, **1996**; b) D. Guillon, *Struct. Bonding (Berlin)* **1999**, *95*, 41–82; c) B. Donnio, D. Guillon, D. W. Bruce, R. Deschenaux, *Metallomesogens In Comprehensive Coordination Chemistry II: From Biology to Nanotechnology*, Vol. 7 (Eds.: J. A. McCleverty, T. J. Meyer, M. Fujita, A. Powell), Elsevier, Oxford, **2003**, Chapter 7.9, pp. 357–627.
- [5] M. Munakata, L. P. Wu, T. Kuroda-Sowa, *Adv. Inorg. Chem.* **1999**, *46*, 173–303.
- [6] K. E. Drexler, *Nanosystems, Molecular Machinery, Manufacturing and Computation*, Wiley, New York, **1992**.
- [7] a) J.-M. Lehn, A. Rigault, J. Siegel, J. Harrowfield, B. Chevrier, D. Moras, *Proc. Natl. Acad. Sci. USA* **1987**, *84*, 2565–2569; b) C. Piguet, G. Hopfgartner, B. Bocquet, O. Schaad, A. F. Williams, *J. Am. Chem. Soc.* **1994**, *116*, 9092–9102; c) T. Suzuki, H. Kotsuki, K. Isobe, N. Moriya, Y. Nakagawa, M. Ochi, *Inorg. Chem.* **1995**, *34*, 530–531; d) E. Psillakis, J. C. Jeffery, J. A. McCleverty, M. D. Ward, *J. Chem. Soc. Dalton Trans.* **1997**, 1645–1651; e) M. Albrecht, R. Fröhlich, *J. Am. Chem. Soc.* **1997**, *119*, 1656–1661; f) T. Hatano, A.-H. Bae, M. Takeuchi, N. Fujita, K. Kaneko, H. Ihara, M. Takafuji, S. Shinkai, *Angew. Chem.* **2004**, *116*, 471–475; *Angew. Chem. Int. Ed.* **2004**, *43*, 465–469.
- [8] a) M. M. Chowdhry, D. M. P. Mingos, A. J. P. White, D. J. Williams, *Chem. Commun.* **1996**, 899–900; b) G. Smith, A. N. Reddy, K. A. Byriel, C. H. L. Kennard, *J. Chem. Soc. Dalton Trans.* **1995**, 3565–3570.
- [9] a) J. Dai, M. Yamamoto, T. Kuroda-Sowa, M. Maekawa, Y. Suenaga, M. Munakata, *Inorg. Chem.* **1997**, *36*, 2688–2690; b) M. Munakata, L. P. Wu, T. Kuroda-Sowa, M. Maekawa, Y. Suenaga, K. Sugimoto, *Inorg. Chem.* **1997**, *36*, 4903–4905.
- [10] a) A. S. Batsanov, M. J. Begley, P. Hubberstey, J. Stroud, *J. Chem. Soc. Dalton Trans.* **1996**, 1947–1957; b) M. Munakata, L. P. Wu, M. Yamamoto, T. Kuroda-Sowa, M. Maekawa, *J. Am. Chem. Soc.* **1996**, *118*, 3117–3124.
- [11] a) D. Whang, Y.-M. Jeon, J. Heo, K. Kim, *J. Am. Chem. Soc.* **1996**, *118*, 11333–11334; b) D. Whang, K. Kim, *J. Am. Chem. Soc.* **1997**, *119*, 451–452; c) D. Whang, K.-M. Park, J. Heo, P. Ashton, K. Kim, *J. Am. Chem. Soc.* **1998**, *120*, 4899–4900; d) S.-G. Roh, K.-M. Park, S. Sakamoto, K. Yamaguchi, K. Kim, *Angew. Chem.* **1999**, *111*, 671–675; *Angew. Chem. Int. Ed.* **1999**, *38*, 638–641.
- [12] D. L. Caulder, K. N. Raymond, *J. Chem. Soc. Dalton Trans.* **1999**, 1185–1200.
- [13] a) J. R. Black, N. R. Champness, W. Levason, G. Reid, *Inorg. Chem.* **1996**, *35*, 4432–4438; b) A. Pfützner, S. Zimmerer, *Angew. Chem.* **1997**, *109*, 1031–1033; *Angew. Chem. Int. Ed. Engl.* **1997**, *36*, 982–984.
- [14] C. Piguet, *J. Inclusion Phenom. Macrocyclic Chem.* **1999**, *34*, 361–391.
- [15] B. Olenyuk, A. Fechtenkötter, P. J. Stang, *J. Chem. Soc. Dalton Trans.* **1998**, 1707–1728.
- [16] O. Mamula, A. Von Zelewsky, G. Bernardinelli, *Angew. Chem.* **1998**, *110*, 302–305; *Angew. Chem. Int. Ed.* **1998**, *37*, 289–293.
- [17] a) J. S. Lindsey, *New J. Chem.* **1991**, *15*, 153–180; b) D. S. Lawrence, T. Jiang, M. Levett, *Chem. Rev.* **1995**, *95*, 2229–2260; c) D. Philp, J. F. Stoddart, *Angew. Chem.* **1996**, *108*, 1243–1286; *Angew. Chem. Int. Ed. Engl.* **1996**, *35*, 1154–1196.
- [18] a) B. Hasenknopf, J. M. Lehn, B. O. Kneisel, G. Baum, D. Fenske, *Angew. Chem.* **1996**, *108*, 1987–1990; *Angew. Chem. Int. Ed. Engl.* **1996**, *35*, 1838–1840; b) M. Schwach, H. D. Hausen, W. Kaim, *Chem. Eur. J.* **1996**, *2*, 446–451; c) C. R. Woods, M. Benaglia, F. Cozzi, J. S. Siegel, *Angew. Chem.* **1996**, *108*, 1985–1987; *Angew. Chem. Int. Ed. Engl.* **1996**, *35*, 1830–1833.
- [19] a) J.-C. Chambron, C. O. Dietrich-Buchecker, J.-P. Sauvage, *Top. Curr. Chem.* **1993**, *165*, 131–162; b) J.-C. Chambron, C. O. Dietrich-Buchecker, V. Heitz, J.-F. Nierengarten, J.-P. Sauvage, *Transition Metals in Supramolecular Chemistry* (Eds.: L. Fabbrizzi, A. Poggi), NATO ASI Series, **1993**, 448, 371–390.
- [20] a) C. Piguet, G. Hopfgartner, B. Bocquet, O. Schaad, A. F. Williams, *J. Am. Chem. Soc.* **1994**, *116*, 9092–9102; b) C. Piguet, G. Hopfgartner, A. F. Williams, J.-C. G. Bünzli, *Chem. Commun.* **1995**, 491–492.
- [21] a) R. Ziessel, D. Matt, L. Toupet, *Chem. Commun.* **1995**, 2033–2034; b) F. M. Romero R. Ziessel, A. Dupont-Gervais, A. Van Dorselaer, *Chem. Commun.* **1996**, 551–552.
- [22] C. L. Hill, X. Zhang, *Nature* **1995**, *373*, 324–326.

- [23] C. P. Collier, E. W. Wong, M. Belohradsky, F. M. Raymo, J. F. Stoddart, P. J. Kuekes, R. S. Williams, J. R. Heath, *Science* **1999**, *285*, 391–394.
- [24] A. El-ghayoury, L. Douce, A. Skoulios, R. Ziessel, *Angew. Chem.* **1998**, *110*, 2327–2331; *Angew. Chem. Int. Ed.* **1998**, *37*, 2205–2208.
- [25] E. C. Constable, *Adv. Inorg. Chem. Radiochem.* **1986**, *28*, 69–121.
- [26] M. Greenwald, D. Wessely, I. Goldberg, Y. Cohen, *New J. Chem.* **1999**, *23*, 337–344.
- [27] a) G. R. Newkome, K. S. Yoo, C. N. Morefield, *Chem. Commun.* **2002**, 2164–2165; b) H. Jiang, S. J. Lee, W. Lin, *Org. Lett.* **2002**, *4*, 2149–2152.
- [28] J.-F. Gohy, B. G. G. Lohmeijer, S. K. Varshney, U. S. Schubert, *Macromolecules* **2002**, *35*, 7427–7435.
- [29] a) U. S. Schubert, C. Eschbaumer, *Angew. Chem.* **2002**, *114*, 3016–3050; *Angew. Chem. Int. Ed.* **2002**, *41*, 2893–2926; b) B. G. G. Lohmeijer, U. S. Schubert, *Angew. Chem.* **2002**, *114*, 3980–3984; *Angew. Chem. Int. Ed. Engl.* **2002**, *41*, 3825–3829.
- [30] Y. Zhang, C. B. Murphy Jr., W. E. Jones, *Macromolecules* **2002**, *35*, 630–636.
- [31] R. Ziessel, L. Douce, A. El-ghayoury, A. Harriman, A. Skoulios, *Angew. Chem.* **2000**, *112*, 1549–1553; *Angew. Chem. Int. Ed.* **2000**, *39*, 1489–1493.
- [32] L. S. Phinheiro, M. L. A. Temperini, *Surf. Sci.* **2000**, *464*, 176–182.
- [33] E. Figgemeier, L. Merz, B. A. Hermann, Y. C. Zimmerman, C. E. Housecroft, H.-J. Güntherodt, E. C. Constable, *J. Phys. Chem. B* **2003**, *107*, 1157–1162.
- [34] P. R. Andres, R. Lunkwitz, G. R. Pabst, K. Böhn, D. Wouters, S. Schmatloch, U. S. Schubert, *Eur. J. Org. Chem.* **2003**, 3769–3776.
- [35] J. Park, A. N. Pasupathy, J. I. Goldsmith, C. Chang, Y. Yaish, J. R. Petta, M. Rinkoski, J. P. Sethna, H. D. Abruna, P. L. McEuen, D. C. Ralph, *Nature* **2002**, *417*, 722–725.
- [36] a) P. J. Carter, C.-C. Cheng, H. H. Thorp, *J. Am. Chem. Soc.* **1998**, *120*, 632–642; b) A. T. Danhner, J. K. Bashkin, *Chem. Commun.* **1998**, 1077–1078.
- [37] M. K. Nazeeruddin, P. Pechy, T. Renouard, S. M. Zakeeruddin, R. Humphry-Baker, P. Comte, P. Liska, L. Cevey, E. Costa, V. Shklover, L. Spiccia, G. B. Deacon, C. A. Bignozzi, M. Grätzel, *J. Am. Chem. Soc.* **2001**, *123*, 1613–1624.
- [38] M. Hissler, A. El-ghayoury, A. Harriman, R. Ziessel, *Coord. Chem. Rev.* **1998**, *180*, 1251–1298.
- [39] R. Ziessel, *Synthesis* **1999**, 1839–1865.
- [40] D.-W. Yoo, S.-K. Yoo, C. Kim, J.-K. Lee, *J. Chem. Soc. Dalton Trans.* **2002**, 3931–3932.
- [41] a) Y. Matsunaga, M. Terada, *Mol. Cryst. Liq. Cryst.* **1986**, *141*, 321–326; b) H. Kawada, Y. Matsunaga, T. Takamura, M. Terada, *Can. J. Chem.* **1988**, *66*, 1867–1871; c) J. Malthête, A.-M. Levelut, L. Liébert, *Adv. Mater.* **1992**, *4*, 37–41; d) D. Pucci, M. Weber, J. Malthête, *Liq. Cryst.* **1996**, *21*, 153–155; e) G. Pickaert, L. Douce, R. Ziessel, D. Guillon, *Chem. Commun.* **2000**, 1584–1585.
- [42] R. Ziessel, G. Pickaert, F. Camerel, B. Donnio, D. Guillon, M. Cesario, T. Prange, *J. Am. Chem. Soc.* **2004**, *126*, 12403–12413.
- [43] K. Hanabusa, M. Yamada, M. Kimura, H. Shirai, *Angew. Chem.* **1996**, *108*, 2086–2088; *Angew. Chem. Int. Ed. Engl.* **1996**, *35*, 1949–1951.
- [44] Y. Yasuda, Y. Takebe, M. Fukumoto, H. Inada, Y. Shirota, *Adv. Mater.* **1996**, *8*, 740–741.
- [45] W. Gu, L. Lu, G. B. Chapman, R. G. Weiss, *Chem. Commun.* **1997**, 543–544.
- [46] R. J. H. Hafkamp, B. P. A. Kokke, I. M. Danke, H. P. M. Geursts, A. E. Rowan, M. C. Feiters, R. J. M. Nolte, *Chem. Commun.* **1997**, 545–546.
- [47] R. A. M. Hikmet, *Mol. Cryst. Liq. Cryst.* **1991**, *198*, 357–370.
- [48] S. M. Kelly, *J. Mater. Chem.* **1995**, *5*, 2047–2057.
- [49] K. Hanabusa, T. Hirita, D. Inoue, M. Kimura, H. Shirai, *Colloids Surf.* **2000**, *169*, 307–316.
- [50] J. Barbera, E. Cavero, M. Lehmann, J.-L. Serrano, T. Sierra, J. T. Vazquez, *J. Am. Chem. Soc.* **2003**, *125*, 4527–4533.
- [51] a) S. D. Hudson, H.-T. Jung, V. Percec, W.-D. Cho, G. Johansson, G. Ungar, V. S. K. Balagurusamy, *Science* **1997**, *278*, 449–452; b) V. Percec, C. M. Michell, W.-D. Cho, S. Uchida, M. Glde, G. Ungar, X. Zeng, Y. Liu, V. S. K. Balagurusamy, P. Heiney, *J. Am. Chem. Soc.* **2004**, *126*, 6078–6094.
- [52] J. Wu, M. D. Watson, L. Zhang, Z. Wang, K. Müllen, *J. Am. Chem. Soc.* **2004**, *126*, 177–186.
- [53] X. Cheng, M. K. Das, U. Baumeister, S. Diele, C. Tschierske, *J. Am. Chem. Soc.* **2004**, *126*, 12930–12940.
- [54] B. Donnio, B. Heinrich, H. Allouchi, J. Kain, S. Diele, D. Guillon, D. W. Bruce, *J. Am. Chem. Soc.* **2004**, *126*, 15258–15268.
- [55] W. D. J. A. Norbert, J. W. Goodby, M. Hird, K. J. Toyne, *Liq. Cryst.* **1997**, *22*, 631–642.
- [56] C. Goze, G. Ulrich, L. Charbonnière, M. Cesario, T. Prangé, R. Ziessel, *Chem. Eur. J.* **2003**, *9*, 3748–3755.
- [57] M. E. Padilla-Tosta, J. M. Lloris, R. M. Martínez-Máñez, A. Benito, J. Soto, T. Pardo, M. A. Miranda, M. D. Marcos, *Eur. J. Inorg. Chem.* **2000**, 741–748.
- [58] a) F. Odobel, J.-P. Sauvage, A. Harriman, *Tetrahedron Lett.* **1993**, *34*, 8113–8116; b) J. P. Collin, A. Harriman, V. Heitz, F. Odobel, J.-P. Sauvage, *J. Am. Chem. Soc.* **1994**, *116*, 5679–5690; c) K. T. Potts, D. Konwar, *J. Org. Chem.* **1991**, *56*, 4815–4816.
- [59] S. Bedel, G. Ulrich, C. Picard, *Tetrahedron Lett.* **2002**, *43*, 1697–1700.
- [60] A. T. Bottini, V. Dev, J. Klink, *Org. Synth.* **1963**, *43*, 6–9.
- [61] F. Camerel, G. Ulrich, R. Ziessel, *Org. Lett.* **2004**, *6*, 4171–4174.
- [62] V. Grosshenny, F. M. Romero, R. Ziessel, *J. Org. Chem.* **1997**, *62*, 1491–1500.
- [63] K. Sonogashira, *Comprehensive Organic Synthesis, Vol. 3* (Eds.: B. M. Trost, L. Fleming, L. A. Paquette), Pergamon, Oxford, **1990**, pp. 545–547.
- [64] P. Davidson, A. M. Levelut, H. Strzelecka, V. Gionis, *J. Phys. Lett.* **1993**, *44*, L-823.
- [65] R. G. Snyder, S. L. Hsu, S. Krimm, *Spectrochim. Acta* **1978**, *34*, 395–406.
- [66] a) X. Du, B. Shi, Y. Liang, *Spectrosc. Lett.* **1999**, *32*, 1–16; b) N. Yamada, T. Imai, E. Koyama, *Langmuir* **2001**, *17*, 961–963, and references therein.
- [67] a) T. Kato, T. Kutsuna, K. Hanabusa, M. Ukon, *Adv. Mater.* **1998**, *10*, 606–608; b) K. Hanabusa, C. Koto, M. Kimura, H. Shirai, A. Kakehi, *Chem. Lett.* **1997**, 429–430.
- [68] R. M. Silverstein, G. C. Bassler, T. C. Morrill, *Spectrometric Identification of Organic Compounds*, Third edition, Wiley, **1976**.
- [69] M. Suzuki, M. Yumoto, M. Kimura, H. Shirai, K. Hanabusa, *Tetrahedron Lett.* **2004**, *45*, 2947–2950.
- [70] a) G. Pickaert, M. Cesario, R. Ziessel, *J. Org. Chem.* **2004**, *69*, 5335–5341. b) CCDC-247669 contains the supplementary crystallographic data for this paper. These data can be obtained free of charge from The Cambridge Crystallographic Data Centre via www.ccdc.cam.ac.uk/data_request/cif.
- [71] C. M. Paleos, D. Tsiourvas, *Angew. Chem.* **1995**, *107*, 1839–1855; *Angew. Chem. Int. Ed. Engl.* **1995**, *34*, 1696.
- [72] C. Tschierske, *J. Mater. Chem.* **2001**, *11*, 2647–2671.
- [73] a) J. J. Van Gorp, J. A. J. M. Vekemans, E. W. Meijer, *J. Am. Chem. Soc.* **2002**, *124*, 14759–14769; b) F. Camerel, C. F. J. Faul, *Chem. Commun.* **2003**, 1958–1959.
- [74] a) Y. Yasuda, E. Lishi, H. Inada, Y. Shirota, *Chem. Lett.* **1996**, 575–576; b) K. Hanabusa, C. Koto, M. Kimura, H. Shirai, A. Kakehi, *Chem. Lett.* **1997**, 429–430; c) M. Kimura, S. Kobayashi, T. Kuroda, K. Hanabusa, H. Shirai, *Adv. Mater.* **2004**, *16*, 335–338.
- [75] a) P. Terech, R. G. Weiss, *Chem. Rev.* **1997**, *97*, 3133–3159; b) L. A. Estroff, A. D. Hamilton, *Chem. Rev.* **2004**, *104*, 1201–1218.
- [76] J. C. P. Gabriel, F. Camerel, P. Batail, P. Davidson, B. Lemaire, H. Desvaux, *Nature* **2001**, *413*, 504–508.
- [77] a) S. Tanaka, M. Shirakawa, K. Kaneko, M. Takeuchi, S. Shinkai, *Langmuir* **2005**, *21*, 2163–2172; b) A. D'Aléo, J.-L. Pozzo, F. Fagest, M. Schmutz, G. Mieden-Gundert, F. Vögtle, V. Caplar, M. Zinic, *Chem. Commun.* **2004**, 190–191.

Received: November 18, 2005
Published online: March 31, 2006